SERBIAN JOURNAL OF ELECTRICAL ENGINEERING
Vol. 5, No. 1, May 2008, 155-170

A Generalized Two Axes Model of a Squirrel-Cage Induction Motor for Rotor Fault Diagnosis

Samir Hamdani[1], Omar Touhami[2], Rachid Ibtiouen[2]

Abstract: A generalized two axes model of a squirrel-cage induction motor is developed. This model is based on a winding function approach and the coupled magnetic circuit theory and takes into account the stator and the rotor asymmetries due to faults. This paper presents a computer simulation and experimental dynamic characteristics for a healthy induction machine, machine with one broken bar and a machine with two broken bars. The results illustrate good agreement between both simulated and experimental results. Also, the power spectral density PSD was performed to obtain a stator current spectrum.

Keywords: Induction machine, Diagnosis, Power spectral density.

1 Introduction

Most electric motor failures interrupt a process, reduce production, and may damage other related machinery. In some factories, very expensive scheduled maintenance is performed in order to prevent sudden motor failures. Therefore, there is a considerable demand to reduce maintenance costs and prevent unscheduled downtimes for electrical drive systems, especially induction motors [1]. Thus, finding efficient and reliable fault diagnostic methods is extremely important. In literature, methods based on analytical models of motor systems are still the most common choices for condition monitoring of the induction machine. Some of these methods are based on a classical model which takes into account the individual conductors in the rotor cage using *R-L* series circuits, with current loops defined by two adjacent rotor bars connected by portions of the end ring. Therefore, for N_r bars, this approach leads to a transient model with a total of $N_r + 3$ differential equations. Such a model is quite complex and computer simulation becomes very long [2,3]. Other methods, based on the *d-q* model suppose that both stator and rotor windings are symmetric and the MMF is sinusoidally distributed. In this model, the equivalent inductance and

[1]USTHB, faculté d'électronique et informatique, BP 32 El Alia Bab Ezzouar, Alger, Algerie;
Email: ham_samir@yahoo.fr
[2]Research Laboratory of Electrotechnics, 10, Av Pasteur El Harrach, Algiers, BP182, 16200 Algeria.

resistance matrix are diagonal. This model is very simple for computer simulation but it can't reflect any winding asymmetries due to the stator or rotor faults [4,5].

In this paper, a new modelling method based on a winding function approach and the coupled magnetic circuit theory [6-8] which takes into account the stator and the rotor asymmetries due to the faults, is presented. The method supposes that both resistances and inductances of the stator are not equal. So, it is possible to introduce any stator asymmetry winding due to faults such as the inter-turn short circuit. The rotor is represented by a N_r loop coupled to each other and to the stator winding, through mutual inductances. For a healthy machine, the rotor loops are identical and have the same parameters, but when a rotor fault occurs, some loops are affected. In this condition, the equivalent resistance and inductance matrix of the stator and the rotor in the two axes model are not diagonal, making this model more generalized than the classical *d-q* model.

2 Generalized Two Axes Model of the Induction Machine

The stator of the machine consists of three sinusoidally distributed windings, displaced by 120°, with N_s equivalent turns, but not necessarily having the same resistance and inductance. The squirrel cage contains N_r bars forming N_r identical loops. Each one consists of two adjacent rotor bars connected by two end ring portions. So, for a cage having N_r bars, there are $2N_r$ nodes and $3N_r$ branches. Therefore, the current distribution can be specified in terms of N_r+1 independent rotor currents. These currents comprise of the N_r rotor loop current i_j $(1 \le j \le N_r)$ plus a circulating current in one of the end rings i_e as illustrated by Fig. 1.

For modelling of the induction machine, the following general assumptions were made:

- negligible saturation;
- uniform air gap;
- stator windings sinusoidally distributed;
- negligible interbar current.

The voltage equations for the stator windings can be written as:

$$\boldsymbol{V}_s = \boldsymbol{R}_s \boldsymbol{I}_s + \frac{\mathrm{d}}{\mathrm{d}t}\boldsymbol{\phi}_s \tag{1}$$

where

$\boldsymbol{V}_s = [v_{s1}, v_{s2}, v_{s3}]^{\mathrm{T}}$ is the stator voltage vector;

$\boldsymbol{I}_s = [I_{s1}, I_{s2}, I_{s3}]^{\mathrm{T}}$ is the stator current vector;

$\boldsymbol{R}_s$ is an 3 by 3 resistance matrix given by:

$$\boldsymbol{R}_s = \begin{bmatrix} R_{s1} & 0 & 0 \\ 0 & R_{s2} & 0 \\ 0 & 0 & R_{s3} \end{bmatrix} \tag{2}$$

$\boldsymbol{\phi}_s = [\phi_{s1}, \phi_{s2}, \phi_{s3}]^{\mathrm{T}}$ is a stator flux linkage vector, witch is given by :

$$\boldsymbol{\phi}_s = \boldsymbol{L}_s \boldsymbol{I}_s + \boldsymbol{M}_{sr} \boldsymbol{I}_r \tag{3}$$

The stator inductance matrix L_s is symmetric with constant elements, it's expression is:

$$\boldsymbol{L}_s = \begin{bmatrix} L_{s1} & M_{s1s2} & M_{s1s3} \\ M_{s2s1} & L_{s2} & M_{s2s3} \\ M_{s3s1} & M_{s3s2} & L_{s3} \end{bmatrix} \tag{4}$$

The mutual inductance M_{sr} is a 3 by N_r matrix consisting of mutual inductances between stator coils and rotor loops, as follows:

$$\boldsymbol{M}_{sr} = \begin{bmatrix} M_{s1r1} & M_{s1r2} & \ldots\ldots & M_{s1rN_r} \\ M_{s2r1} & M_{s2r2} & \ldots\ldots & M_{s2rN_r} \\ M_{s3r1} & M_{s3r2} & \ldots\ldots & M_{s3rN_r} \end{bmatrix} \tag{5}$$

$\boldsymbol{I}_r = [I_{r1}, I_{r2}, \ldots, I_{rN_r}]$ is the rotor current vector ; each element I_j represents the current loop.

A change of variables which formulates transformation of the 3-phase stator variables and N_r rotor variables to the arbitrary two axes reference may be done by the use of $\boldsymbol{K}_s$ and $\boldsymbol{K}_r$ transformation matrixes, respectively given by:

$$\boldsymbol{K}_s = \sqrt{\frac{2}{3}} \begin{bmatrix} \sin(\theta) & \sin\left(\theta - \frac{2\pi}{3}\right) & \sin\left(\theta + \frac{2\pi}{3}\right) \\ \cos(\theta) & \cos\left(\theta - \frac{2\pi}{3}\right) & \cos\left(\theta + \frac{2\pi}{3}\right) \end{bmatrix} \tag{6}$$

$$\boldsymbol{K}_r = \sqrt{\frac{2}{N_r}} \begin{bmatrix} \sin\left(\theta - \theta_r - \dfrac{p\alpha_r}{2}\right) & \cdots & \sin\left(\theta - \theta_r - \dfrac{p(2j-1)\alpha_r}{2}\right) \\ \sin\left(\theta - \theta_r - \dfrac{p\alpha_r}{2}\right) & \cdots & \sin\left(\theta - \theta_r - \dfrac{p(2j-1)\alpha_r}{2}\right) \end{bmatrix} \tag{7}$$

where $\theta = \omega t$, $\theta_r = \omega_r t$ is the two axes reference angular velocity, ω_r is the rotor angular velocity. By the use of $\boldsymbol{K}_S$, the stator voltage can be written as:

$$\boldsymbol{V}_{dq}^{s} = \boldsymbol{K}_s \boldsymbol{R}_s \boldsymbol{K}_s^{-1} \boldsymbol{I}_{dq}^{s} + \boldsymbol{K}_s \frac{\mathrm{d}}{\mathrm{d}t} (\boldsymbol{K}_s^{-1} \boldsymbol{\phi}_{dq}^{s}) . \tag{8}$$

By development of this expression, it is possible to find the electric equation of the stator in the two axes reference. This equation is given by:

$$\boldsymbol{V}_{dq}^{s} = \boldsymbol{R}_{dq}^{s} \boldsymbol{I}_{dq}^{s} + \omega \begin{bmatrix} 0 & -1 \\ 1 & 0 \end{bmatrix} \boldsymbol{\phi}_{dq}^{s} + \frac{\mathrm{d}}{\mathrm{d}t} \boldsymbol{\phi}_{dq}^{s} \tag{9}$$

where $\boldsymbol{R}_{dz}^{s}$ is the equivalent resistance matrix, it's given by:

$$\boldsymbol{R}_{dq}^{s} = \begin{bmatrix} R_{ds} & \mathrm{R}_{\mathrm{dqs}} \\ R_{dqs} & \mathrm{R}_{\mathrm{qs}} \end{bmatrix} . \tag{10}$$

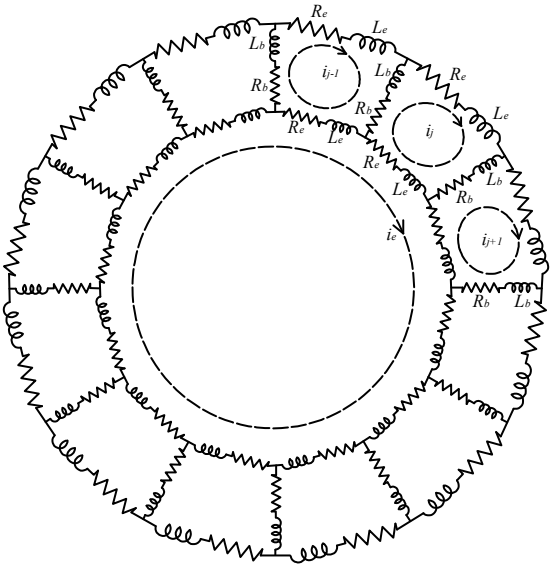

Fig. 1 – *Rotor cage representation*.

where

$$R_{ds} = \frac{1}{2}(R_{s2} + R_{s3}),$$
$$R_{qs} = \frac{2}{3}R_{s1} + \frac{1}{6}(R_{s2} + R_{s3}), \tag{11}$$
$$R_{dqs} = \frac{1}{2\sqrt{3}}(R_{s2} - R_{s3}).$$

In the same manner, the flux equation can be written as:

$$\boldsymbol{\phi}_{dq}^{s} = \boldsymbol{L}_{dq}^{s}\boldsymbol{I}_{dq}^{s} + \boldsymbol{M}_{dq}^{sr}\boldsymbol{I}_{dq}^{r}, \tag{12}$$

with:

$$\boldsymbol{L}_{dq}^{s} = \boldsymbol{K}_{s}\boldsymbol{L}_{s}\boldsymbol{K}_{s}^{-1} = \begin{bmatrix} L_{ds} & L_{dqs} \\ L_{dqs} & L_{qs} \end{bmatrix}. \tag{13}$$

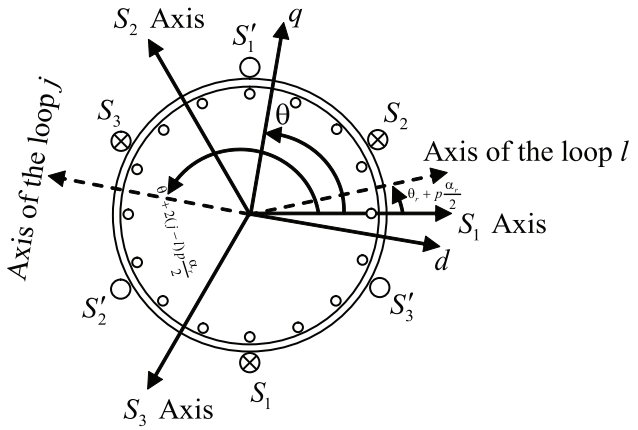

Fig. 2 – *Two axes reference frame.*

Note that for a healthy induction motor, the stator windings are identical and have the same resistance and inductance ($R_{s1} = R_{s2} = R_{s3} = R_s$, $L_{s1} = L_{s2} = L_{s3} = L_s$), the equivalent resistance and inductance matrix $\boldsymbol{R}_{dq}^{s}$ and $\boldsymbol{L}_{dq}^{s}$ will be diagonal:

$$\boldsymbol{R}_{dq}^{s} = \begin{bmatrix} R_s & 0 \\ 0 & R_s \end{bmatrix}, \tag{14}$$

$$\boldsymbol{L}_{dq}^{s} = \begin{bmatrix} L_s & 0 \\ 0 & L_s \end{bmatrix}. \tag{15}$$

$\boldsymbol{M}_{dq}^{sr}$ is the equivalent mutual inductance matrix between the stator windings and the rotor loops. This matrix is given by:

$$\boldsymbol{M}_{dq}^{sr} = \boldsymbol{K}_s \boldsymbol{M}_{sr} \boldsymbol{K}_r^{-1} = \begin{bmatrix} M_d & \mathrm{M}_{dq} \\ M_{dq} & \mathrm{M}_q \end{bmatrix}. \tag{16}$$

From the rotor cage equivalent circuit represented by Fig. 1, the electric equation of the j-th loop can be defined as:

$$0 = 2(R_b + R_e) i_j - R_b i_{(j-1)} - R_b i_{(j+1)} + \frac{\mathrm{d}\phi_{rj}}{\mathrm{d}t}. \tag{17}$$

ϕ_{rj} is the flux crossing the rotor loop j, it represents the sum of the flux due to stator currents and the flux due to the rotor loop. The expression of ϕ_{rj} is given by:

$$\phi_{rj} = (L_{rp} + 2(L_b + L_e)) i_j + \sum_{\substack{k=1 \\ k \neq j}}^{Nr} M_{rr} + \sum_{k=1}^{3} M_{rjsk} i_{sk} - L_b i_{(j-1)} - L_b i_{(j+1)} i_k \,. \tag{18}$$

Thus, the rotor electric equation can be written as:

$$0 = \boldsymbol{R}_r \boldsymbol{I}_r + \frac{\mathrm{d}}{\mathrm{d}t} \boldsymbol{\phi}_r \tag{19}$$

where $\boldsymbol{R}_r$ is the equivalent rotor loop resistance matrix, its expression is given by :

$$\boldsymbol{R}_r = \begin{bmatrix} 2(R_b + R_e) & -R_b & \cdots & -R_b \\ -R_b & 2(R_b + R_e) - R_b & \cdots & 0 \\ \vdots & \vdots & \ddots & \vdots \\ -R_b & 0 & \vdots & 2(R_b + R_e) \end{bmatrix}. \tag{20}$$

R_b and R_e are: the bar resistance and the end-ring segment resistance, respectively. $\boldsymbol{\phi}_r = [\phi_{r1}, \phi_{r2}, \ldots, \phi_{rN_r}]$ represents the rotor loop flux vector:

$$\boldsymbol{\phi}_r = \boldsymbol{L}_r \boldsymbol{I}_r + \boldsymbol{M}_{rs} \boldsymbol{I}_s \tag{21}$$

where $\boldsymbol{L}_r$ is a $N_r \times N_r$ inductance matrix of rotor loops given by (22):

$$\boldsymbol{L}_r = \begin{bmatrix} L_{rp} + 2(L_b + L_e) & M_{rr} - L_b & M_{rr} & \cdots & M_{rr} - L_b \\ M_{rr} - L_b & L_{rp} + 2(L_b + L_e) & M_{rr} - L_b & \cdots & M_{rr} \\ M_{rr} & M_{rr} - L_b & \ddots & \ddots & \vdots \\ \vdots & \ddots & \ddots & \ddots & \vdots \\ M_{rr} - L_b & \cdots & M_{rr} & \cdots & L_{rp} + 2(L_b + L_e) \end{bmatrix} \tag{22}$$

L_b is the rotor bar leakage inductance, L_e is the end-ring segment inductance and $\boldsymbol{M}_{rs} = \boldsymbol{M}_{sr}^{\mathrm{T}}$. Transformations (6) and (7) applied to electrical equations of the rotor loop give:

$$0 = \boldsymbol{R}_{dq}^{r}\boldsymbol{I}_{dq}^{r} + (\omega - \omega_r)\begin{bmatrix} 0 & -1 \\ 1 & 0 \end{bmatrix}\boldsymbol{\phi}_{dq}^{r} + \frac{\mathrm{d}}{\mathrm{d}t}\boldsymbol{\phi}_{dq}^{r}, \tag{23}$$

where $\boldsymbol{\phi}_{dq}^{r} = \boldsymbol{L}_{dq}^{r}\boldsymbol{I}_{dq}^{r} + \boldsymbol{M}_{dq}^{rs}\boldsymbol{I}_{dq}^{s}$, $\boldsymbol{M}_{dq}^{rs} = (\boldsymbol{M}_{dq}^{sr})^{\mathrm{T}}$ and:

$$\boldsymbol{R}_{dq}^{r} = \begin{bmatrix} R_{dr} & R_{dqr} \\ R_{dqr} & R_{qr} \end{bmatrix}, \tag{24}$$

$$\boldsymbol{L}_{dq}^{r} = \begin{bmatrix} L_{dr} & L_{dqr} \\ L_{dqr} & L_{qr} \end{bmatrix}. \tag{25}$$

$\boldsymbol{R}_{dq}^{r}$, $\boldsymbol{L}_{dq}^{r}$ and $\boldsymbol{M}_{dq}^{rs}$ represent the rotor resistance matrix, the rotor loop inductance matrix and the coupling inductance matrix between the rotor loops and stator coils, respectively. Considering (9) and (23), one can write the general expression of the squirrel induction motor in the two axes reference frame given in (26) as:

$$\begin{bmatrix} V_{dq}^{s} \\ 0 \end{bmatrix} = \boldsymbol{R}\begin{bmatrix} I_{dq}^{s} \\ I_{dq}^{r} \end{bmatrix} + \boldsymbol{K}\begin{bmatrix} \phi_{dq}^{s} \\ \phi_{dq}^{r} \end{bmatrix} + \frac{\mathrm{d}}{\mathrm{d}t}\begin{bmatrix} \phi_{dq}^{s} \\ \phi_{dq}^{r} \end{bmatrix}, \tag{26}$$

where:

$$\boldsymbol{R} = \begin{bmatrix} R_{dq}^{s} & 0 \\ 0 & R_{dq}^{r} \end{bmatrix} \tag{27}$$

$$\boldsymbol{K} = \begin{bmatrix} 0 & -\omega & 0 & 0 \\ \omega & 0 & 0 & 0 \\ 0 & 0 & 0 & -(\omega - \omega_r) \\ 0 & 0 & (\omega - \omega_r) & 0 \end{bmatrix} \tag{28}$$

$$\begin{bmatrix} \phi_{dq}^{s} \\ \phi_{dq}^{r} \end{bmatrix} = \boldsymbol{L}\begin{bmatrix} I_{dq}^{s} \\ I_{dq}^{r} \end{bmatrix} \tag{29}$$

with:

$$\boldsymbol{L} = \begin{bmatrix} L_{dq}^{s} & M_{dq}^{sr} \\ M_{dq}^{rs} & L_{dq}^{r} \end{bmatrix} \tag{30}$$

In order to obtain the healthiest possible simulation, it is convenient to avoid the derivative function and use only integral functions. However, the stator and rotor currents can be obtained according to the flux by:

$$\begin{bmatrix} I_{dq}^{s} \\ I_{dq}^{r} \end{bmatrix} = \boldsymbol{L}^{-1} \begin{bmatrix} \phi_{dq}^{s} \\ \phi_{dq}^{r} \end{bmatrix} \tag{31}$$

Finally, substituting (31) into (26) yields:

$$\frac{\mathrm{d}}{\mathrm{d}t} \begin{bmatrix} \phi_{dq}^{s} \\ \phi_{dq}^{r} \end{bmatrix} = \begin{bmatrix} V_{dq}^{s} \\ 0 \end{bmatrix} - (\boldsymbol{R}\boldsymbol{L}^{-1} + \boldsymbol{K}) \begin{bmatrix} \phi_{dq}^{s} \\ \phi_{dq}^{r} \end{bmatrix}. \tag{32}$$

Note that the inductance matrix L depends on the rotor angle position θ_r, it will be necessary to update and reverse it at each calculation step of the simulation. For the mechanical equation, it can be written as:

$$\frac{\mathrm{d}}{\mathrm{d}t}\omega_r = \frac{p}{J}(T_e - T_L) \tag{33}$$

where T_L is the load torque; T_e is the electromagnetic torque, it can be expressed as partial variation of the co-energy with respect to the rotor position [5].

$$T_e = (\boldsymbol{K}_s^{-1}\boldsymbol{I}_{dq}^{s})^{\mathrm{T}} \frac{\mathrm{d}M_{sr}}{\mathrm{d}\theta_r} (\boldsymbol{K}_r^{-1}\boldsymbol{I}_{dq}^{r}). \tag{34}$$

Equations (32-34) describe the squirrel induction motor model in the generalized two axes reference frame. With this model it will be possible to modify stator and rotor parameters of the motor in order to consider some faults such as: the inter-turn short circuit and the rotor loop bars and end-ring defaults.

3 Calculation of the Inductance for a Healthy Induction Motor

The inductances are calculated by means of a winding function. According to this theory and for a constant air-gap, the mutual inductance between any two windings ' i' and ' j' is given by [6]:

$$M_{ij} = \frac{\mu_0 \ell r}{g} \int_0^{2\pi} N_i(\theta_r, \varphi) N_j(\theta_r, \varphi) \mathrm{d}\varphi. \tag{35}$$

$N_i(\theta_r, \varphi)$ and $N_j(\theta_r, \varphi)$ are the winding function of the 'i' and 'j' coil, respectively. They represent the spatial distribution of the MMF along the air-gap for a unit current circulating in the winding [5], [6]. This function depends on the spatial position of any point along the air-gap defined by φ and the rotor angular position compared to a given reference defined by θ_r.

Consider the stator windings disposition shown by Fig. 3. Taking as a reference the magnetic axis of the first phase, the normalized stator winding function for this phase is:

$$N_{s1} = \frac{N_s}{2}\cos\varphi \tag{36}$$

Substituting (36) into (35), one can deduce the magnetizing inductance for each stator coil as:

$$L_{ms} = \frac{\mu_0 \ell r N_s^2 \pi}{4g} \tag{37}$$

The total inductance of the stator coil is the sum of the magnetizing inductance L_{ms} and the leakage inductance L_{sf}. However, one can write for a symmetric stator winding:

$$L_{s1} = L_{s2} = L_{s3} = L_{sf} + L_{ms} \tag{38}$$

where l is the stack length, r is the average radius of the air-gap, g is the radial air-gap length and N_s is the number of turns of the stator coil. The mutual inductance of two stator coils 'i' and 'j' $(i \neq j)$ is given by:

$$M_{sisj} = \frac{-L_{ms}}{2}. \tag{39}$$

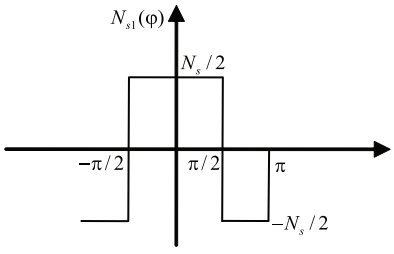

Fig. 3 – *Winding distribution of the first stator coil.*

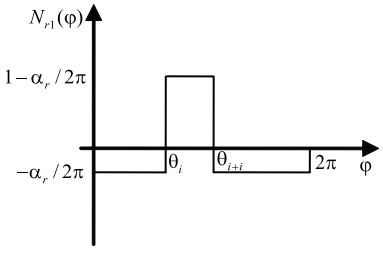

Fig. 4 – *Winding distribution of the rotor loop.*

Fig. 4 shows the function winding of a rotor loop related to a given rotor position. θ_i and θ_{i+1} indicate the position of the two bars which form the rotor loop. This function is defined by:

$$N_{ri}(\varphi) = \begin{cases} -\dfrac{\alpha_r}{2\pi} & 0 \le \varphi \le \theta_i \\ 1-\dfrac{\alpha_r}{2\pi} & \theta_i \le \varphi \le \theta_{i+1} \\ -\dfrac{\alpha_r}{2\pi} & \theta_{i+1} \le \varphi \le 2\pi \end{cases} \tag{40}$$

Substituting (36) and (40) in (35), the mutual inductance between a stator winding '*j*' and a rotor loop '*i*' is expressed by:

$$M_{sirj} = L_m \cos\left(\theta_r + \frac{p(2i-1)}{2} - (j-1)\frac{2\pi}{3}\right), \tag{41}$$

where:

$$L_m = L_{ms}\frac{4\sin\left(\frac{\alpha_r}{2}\right)}{\pi N_s}. \tag{42}$$

The rotor loop inductance L_{rp} and the mutual inductance between two rotor loops are respectively given by:

$$L_{rp} = \frac{\mu_0 \ell r \alpha_r}{g}\left(1 - \frac{\alpha_r}{2\pi}\right), \tag{43}$$

$$M_{rr} = \frac{\mu_0 \ell r}{g}\left(-\frac{\alpha_r^2}{2\pi}\right). \tag{44}$$

4 Calculation of the Inductance for an Induction Motor with N_{bc} Bars Broken

A squirrel cage induction machine with rotor bars in default is represented by Fig. 5. Consider N_{bc} to be the number of adjacent broken bars. The winding function distribution corresponding to the equivalent loop is shown in Fig. 6. For this loop, calculation of the inductance led to the following expression:

$$L_{rp} = \frac{\mu_0 \ell r \alpha_r}{g}\left((N_{bc}+1) - (2N_{bc}+1)\frac{\alpha_r}{2\pi}\right). \tag{45}$$

The mutual inductance between this loop and all other loops not affected by the fault is:

$$M_{rr} = \frac{\mu_0 \ell r}{g}\left(\frac{\alpha_r^2}{2\pi}\right)\left(N_{bc}+1\right). \tag{46}$$

In the same manner, one can deduce the mutual inductance between a stator coil '*j*' and the faulty loop denoted '*i*' as:

$$M_{sird} = \frac{\mu_0 \ell r}{g} N_s \cos\left(\theta_r + \frac{p(2i+N_{bc}-1)\alpha_r}{2} - (j-1)\frac{2\pi}{3}\right)\sin\left((N_{bc}+1)\frac{\alpha_r}{2}\right). \tag{47}$$

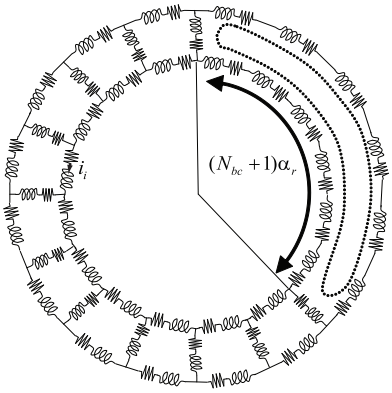

Fig. 5 – *Representation of* N_{bc} *broken bars*.

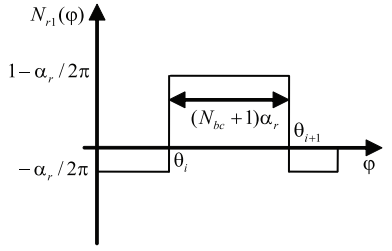

Fig. 6 – *Winding distribution for* N_{bc} *bars broken*.

5 Simulation and Experimental Results

To simulate the squirrel cage induction machine model, a computer program written in MATLAB was used. The differential equations were resolved using the fourth order Runge-Kutta method. First, the developed model was used to simulate a healthy and faulty 4kW squirrel cage induction machine with the specified parameters given in the appendix. To validate the proposed model, the experimental setup represented by Figs. 7 and 8 was designed and built. This test setup consisted of an industrial induction motor coupled to a DC generator acting as a load and a data acquisition system.

As shown in Fig. 9, two induction motors of the same type but with different faults were available in addition to a healthy machine. The first had one bar broken and the second had two broken bars. The stator current and voltage were measured via LA-55P current sensors and LV-25M voltage sensors, respectively as shown in Fig. 10. Each measured signal was simultaneously sampled through channels of a 16 bit 200kHz PCI data acquisition (DAQ) board and stored directly into a desktop computer. Once the data acquisition was complete, a Matlab program was used to process and analyze the data.

Figs. 11, 12 and 13 show simulation and experimental results of the instantaneous stator current and speed during start -up for the cases of a healthy machine, a machine with one broken bar and a machine with two broken bars. These results were obtained for a sinusoidal voltage supply with a constant load.

The simulation and the experimental results are not exactly the same but a good agreement is noted between them. The reasons for the differences were assumed to be caused by the assumptions used in the model and slight errors in setting particular parameter values. For example, one of the assumptions was that the rotor bar current is zero if a bar is broken. In practice, however, there may be a current path through laminations between adjacent bars. This effect would lead to a decrease in the stator phase current modulation and therefore could account for the differences between the simulated and measured stator phase currents. Similarly, it is difficult to estimate exact values for the model parameters (such as bar resistance, self-inductance and mutual-inductance). Errors in the setting of these parameters could also contribute to the differences between simulated and measured results.

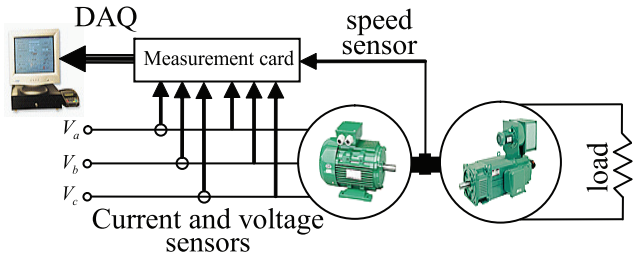

Fig. 7 – *Diagram of the experimental setup.*

Fig. 8 – *Photo of the experimental setup.*

Fig. 9 – *Rotors under test.*

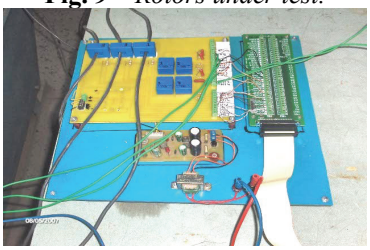

Fig. 10 – *Current and voltage sensor board.*

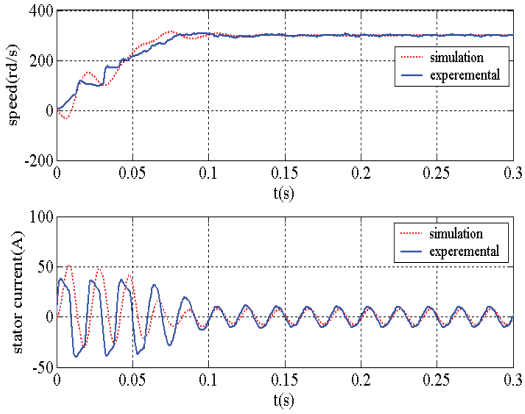

Fig. 11 – *Speed and current for a healthy machine.*

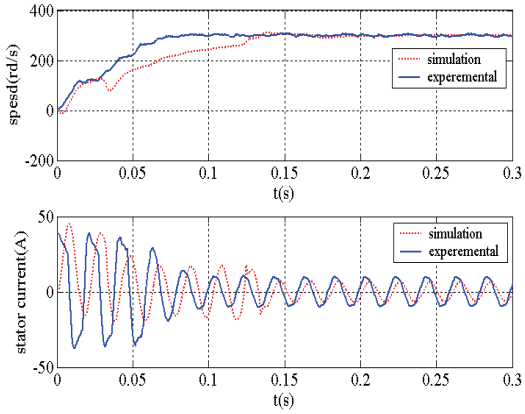

Fig. 12 – *Speed and current for a machine with one bar broken.*

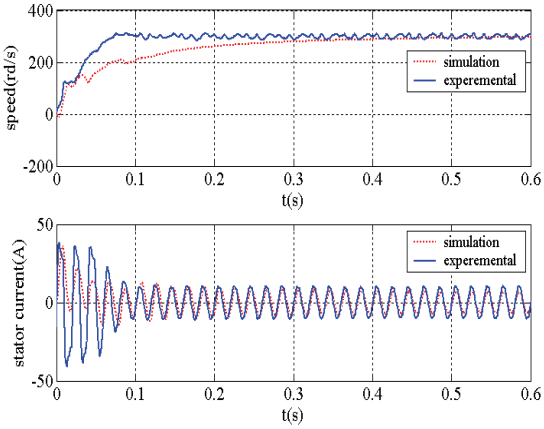

Fig. 13 – *Speed and current for a machine with two bars broken.*

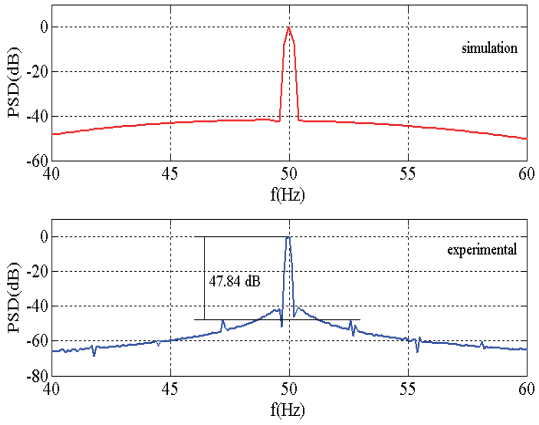

Fig. 14 – *Power spectral density for a healthy machine.*

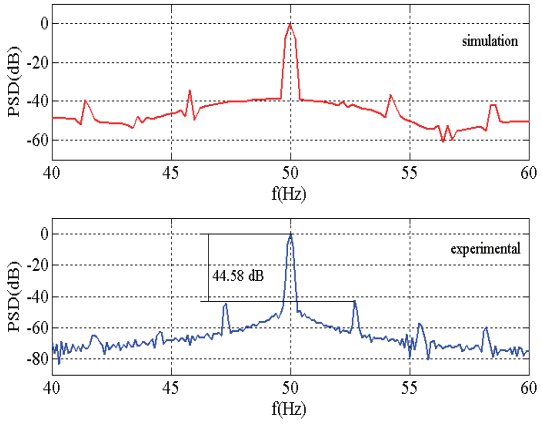

Fig. 15 – *Power spectral density for a machine with one bar broken.*

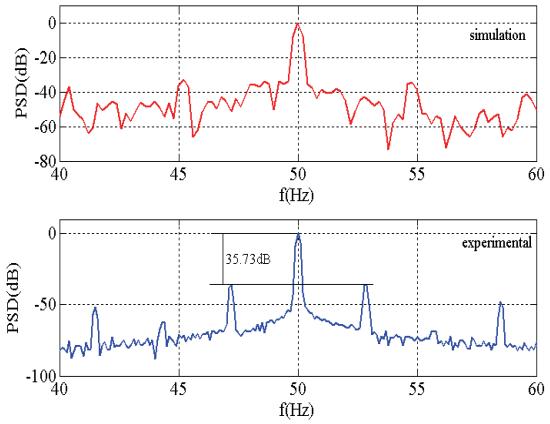

Fig. 16 – *Power spectral density for a machine with two bars broken.*

In order to extract more information from the stator current wave, the power spectral density PSD was used to highlight the appearance of $(1 \pm 2ks) f_s$ frequencies components near the fundamental one. Figs. 14, 15 and 16 show simulation and experimental stator current PSD values for a healthy machine, a machine with one broken bar and a machine with two bars broken. One can notice the appearance of harmonic components in the right and left sideband of the fundamental with frequencies corresponding exactly to the mathematical relation $(1 \pm 2ks) f_s$ where f_s is the fundamental frequency and s is the slip.

As shown, the fault-related spectral components tend to grow with the extent of the fault. For experimental results the amplitude of the first right and left sideband is -52dB, -44 dB and -36dB for a healthy machine, a machine with one broken bar and a machine with two broken bars, respectively. In simulation results, only the fundamental component is present in the spectrum of a healthy machine. For the two other machines the amplitude of the right and the left sideband is: -43dB and -50dB.

6 Conclusion

A generalized two axes approach to squirrel cage induction machine modelling has been presented. The model is based on a winding function approach and the coupled magnetic circuit theory and takes into account the stator and the rotor asymmetries due to faults. The model is used to simulate the behaviour of a healthy and faulty machine and it is validated by experimental results. The dynamic characteristics of induction motors under different conditions obtained by computer simulation are in good agreement with those obtained experimentally. The spectrum analysis of the stator current showed the

existence of harmonic components in the sideband of the fundamental with frequencies corresponding exactly to the relation $(1 \pm 2ks) f_s$.

7 Appendix

Squirrel cage induction machine parametes:

$P_n = 4\,\text{kW}$; $V_n = 220/380\,\text{V}$; (Δ/Y) ; $I_n = 15.2/8.8\,\text{A}$;

$N_n = 1435\,\text{tr/mn}$; $p = 2$; $f = 50\,\text{Hz}$; $\cos\varphi = 0.83$;

$J = 0.002\,\text{kg m}^2$; $R_s = 1.5\,\Omega$; $L_s = 7\,\text{mH}$; $L_{ms} = 0.55\,\text{H}$; $L_{ss} = 0.54\,\text{H}$;

$L_b = 0.28\,\mu\text{H}$; $R_b = 96.940.036\,\mu\Omega$;

$R_e = 5\,\mu\Omega$; $L_e = 0.036\,\mu\text{H}$;

$N_r = 28$; $r = 70\,\text{mm}$; $g = 0.28\,\text{mm}$; $l = 120\,\text{mm}$; $N_s = 156$.

8 References

[1] M. Haji, H.A. Toliyat: Pattern Recognition - A Technique for Induction Machines Rotor Broken Bar Detection, IEEE Trans. On Ener. Conv. Vol. 16, No. 2, Dec. 2001, pp. 312-317.

[2] C.C.M. Cunha, R.O.C. Lyra, B. C. Filho: Simulation and Analysis of Induction Machines with Rotor Asymmetries, IEEE Trans. Ind. Appl., Vol. 41, No. 1, Jan/Feb 2005, pp. 18-24.

[3] S.J. Manolas, J.A. Tegopoulos: Analysis of Squirrel Cage Induction Motors with Broken Bars and Rings, IEEE Trans. on Ener. Conv., Vol. 14, No. 4, Dec. 1999, pp. 1300-1305.

[4] Y. Zhao, T.A. Lipo: Modeling and Control of a Multi-phase Induction Machine with Structural Unbalance, IEEE Trans. on Ener. Conv., Vol. 11, No. 3, Sep. 1996, pp. 570-577.

[5] G. Didier, H. Razik: Sur la detection d'un defaut au rotor des moteurs asynchrones, 3EI, No. 27, Déc. 2001, pp. 1-10.

[6] A.R. Munoz, T.A. Lipo: Complex Vector Model of the Squirrel-cage Induction Machine Including Instantaneous Rotor Bar Currents, IEEE Trans. Ind. Appl, Vol. 35, No. 6, Nov/Dec 1999, pp. 1332-1340.

[7] X.L.Y. Liao, H.A. Toliyat, A.E. Antably, T.A. Lipo: Multiple Coupled Circuit Modeling of Induction Machines, IEEE Trans. Ind. Appl, Vol. 31, No. 2, Mar/Apr 1995, pp. 311-317.

[8] H.A. Toliyat, T.A. Lipo: Transient Analysis of Cage Induction Machines Under Stator, Rotor Bar and End Ring Faults, IEEE Trans. on Ener. Conv., Vol. 10, No. 2, June 1995, pp. 241-247.